Cu2ZnSnS4 Hierarchical Microspheres as an Effective Counter Electrode Material for Quantum Dot Sensitized Solar Cells

ARTICLE *in* THE JOURNAL OF PHYSICAL CHEMISTRY C · SEPTEMBER 2012

Impact Factor: 4.77 · DOI: 10.1021/jp306628m

THE JOURNAL OF PHYSICAL CHEMISTRY C

Article

pubs.acs.org/JPCC

Cu_2ZnSnS_4 Hierarchical Microspheres as an Effective Counter Electrode Material for Quantum Dot Sensitized Solar Cells

Jun Xu, Xia Yang, Qing-Dan Yang, Tai-Lun Wong, and Chun-Sing Lee*

Department of Physics and Materials Science, and Center of Super-Diamond and Advanced Films (COSDAF), City University of Hong Kong, Hong Kong SAR, P. R. China

Supporting Information

ABSTRACT: We explore the application of Cu_2ZnSnS_4 (CZTS) microspheres as an effective counter electrode material for low-cost and high-efficiency quantum dot sensitized solar cells (QDSSCs). Nearly monodisperse Cu_2ZnSnS_4 (CZTS) hierarchical microspheres with diameters of ~2 μm built from nanoflakes have been synthesized via a facile solvothermal approach. The nanoflakes are assembled from CZTS quantum dots with 3−5 nm, showing a three-tiered organization of hierarchical microspheres. The morphology, crystal structure, composition, and optical properties of the CZTS microspheres are characterized by SEM, HRTEM, XRD, XPS, EDS, EELS, Raman, and UV−vis analysis. Chemical conversion and phase transformation from hexagonal CuS to tetragonal CZTS have been systematically investigated to reveal formation mechanism of the CZTS microspheres. These CZTS microspheres are used as an effective counter electrode material in QDSSCs for the first time to show high electrocatalytic activity for catalyzing reduction of polysulfide (S^{2-}/S_n^{2-}) electrolyte, contributing to significant improvement in short current density (J_{SC}) and fill factor (FF). A solar cell using the CZTS microspheres-coated FTO (SnO_2:F) glass substrate as a counter electrode achieves a power conversion efficiency (PCE) of 3.73% under AM 1.5G illumination with an intensity of 100 mW cm^{-2}, which is much higher than that (0.33%) of the cell using the bare FTO glass substrate as a counter electrode and is also higher than that (2.27%) of the cell using the noble Pt-coated FTO glass substrate as a counter electrode.

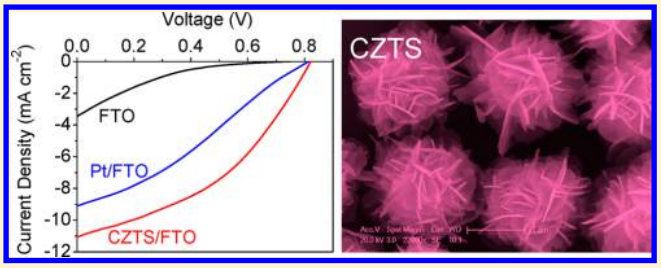

1. INTRODUCTION

Exploration of novel nanostructures is a promising approach to meet the performance demand for low-cost solar cells. The higher-order organization of smaller nanocrystals into complex hierarchical architectures across extended length scales opens up new opportunities to develop materials with novel properties and efficient applications.[1−5] Hierarchical architectures with nanometer-to-micrometer dimensions, which have been reported to show widespread potential applications in catalysis and chemical sensing,[6−10] are promising candidate structures for an effective counter electrode. The counter electrode in photoelectrochemical (PEC) solar cells plays an important role in transferring electrons from the external circuit back to redox electrolyte for catalytic reduction of the redox electrolyte.[11−14] A counter electrode of hierarchical structures with a large roughness factor (RF) is considered to be beneficial for providing a large interfacial contact area and thus more efficient charge transfer to the electrolyte.[14]

The Cu_2ZnSnS_4 (CZTS) compound is one of the most promising candidates for low-cost photovoltaic materials, for the abundances of its constituting elements, low toxicity, a suitable energy band gap (~1.5 eV), and a high absorption coefficient (~10^4 cm^{-1}).[15−19] Thin film of CZTS has been recently applied as an effective photocathode material to replacing platinum in low-cost dye-sensitized solar cells (DSSCs).[20,21] For example, Lin et al. have reported the application of a selenized CZTS film as an effective counter electrode in DSSCs. The device shows good electrocatalytic performance for regeneration of iodide from triiodide in a redox electrolyte (I^-/I_3^-) and delivers a power conversion efficiency (PCE) of 7.37%, which is comparable to that (7.04%) of the cell with a Pt counter electrode (4.7% increase in efficiency).[20] Recently, quantum dot sensitized solar cells (QDSSCs) have been widely developed as low-cost and high theoretic efficiency photovoltaic devices to replace the costly dyes in DSSCs.[11,22−25] However, to the best of our knowledge, there is so far no report on the electrocatalytic performance of CZTS as a counter electrode in QDSSCs.

In this work, we report a facile solvothermal method for preparing nearly monodisperse CZTS hierarchical microspheres with a three-tiered organization (nanocrystallites → nanoflakes → microspheres). The evolution process of the hierarchical CZTS structures is investigated to reveal their formation mechanism. These CZTS microspheres are further demonstrated as an effective counter electrode material in QDSSCs for the first time to show high electrocatalytic activity

Received: July 4, 2012
Revised: August 12, 2012
Published: August 28, 2012

   dx.doi.org/10.1021/jp306628m | J. Phys. Chem. C 2012, 116, 19718−19723

for the reduction of polysulfide (S^{2-}/S_n^{2-}) electrolyte, yielding a PCE of 3.73%, which shows 64.3% improvement in efficiency compared to the cells using a Pt counter electrode with an efficiency of 2.27%.

2. EXPERIMENTAL SECTION

2.1. Synthesis of CZTS Microspheres. In a typical synthesis, 0.5 mmol of $Cu(NO_3)_2$, 0.25 mmol of $Zn(NO_3)_2$, and 0.25 mmol of $SnCl_4$ were dissolved in 40 mL of triethylene glycol (TEG), followed by addition of 1.25 mmol of S powder with ultrasonication for 30 min. The mixed solution was then kept at 250 °C for 48 h. After naturally cooled to room temperature, the reaction product was collected, washed with absolute ethanol for several times, and then dried under vacuum.

2.2. Synthesis of ZnO/ZnSe/CdSe Nanocable Arrays. Arrays of ZnO/ZnSe/CdSe nanocables grown on FTO (F:SnO_2) substrates were prepared by a successive ions-exchange method using ZnO nanowire arrays as precursors due to the large solubility product constant (K_{sp}) difference among ZnO, ZnSe, and CdSe.[26,27] In a typical preparation, arrays of ZnO nanowires on FTO glass substrates were prepared by reacting ZnO-seeded FTO substrates in a mixed aqueous solution of $Zn(NO_3)_2$ (25.0 mM) and hexamethylenetetramine (25.0 mM) at 92 °C for about 3 h to grow ZnO nanowires. This growth was repeated for about 10 times to get a desirable length of the ZnO nanowires. These arrays of ZnO nanowires on FTO substrates were annealed in air at 400 °C for 30 min for improving their crystallinity and removal of impurities. Arrays of ZnO/ZnSe core/shell nanocables were then synthesized by immersing these ZnO nanowire arrays in a Se^{2-} ion solution (6.0 mM) prepared by reacting Se powder with $NaBH_4$ and kept at 55 °C for about 3 h. Arrays of trilayer ZnO/ZnSe/CdSe core/shell nanocables were prepared by further reacting these ZnO/ZnSe nanocable arrays with a $Cd(NO_3)_2$ solution (25.0 mM) at 55 °C for 10 h. The samples were washed with deionized water and finally dried in a nitrogen flow.

2.3. Solar Cell Fabrications. The as-prepared CZTS microspheres were dispersed in ethanol and then deposited on FTO glass substrates (14 Ω per square) via a spin-coating method with a rotational speed of 800 rpm. The CZTS-coated FTO (CZTS/FTO) glass substrates were annealed in nitrogen at 400 °C for 30 min and used as counter electrodes. To examine the effects of different counter electrodes, Pt-coated FTO (Pt/FTO) counter electrodes were also prepared by dipping the FTO glass in a H_2PtCl_4 ethanol solution (8 mM) and blow-dried with nitrogen gas. After repeating the dip-and-dry cycle for 5 times, the samples were annealed in air at 400 °C for 20 min. A solar cell was prepared by assembling and bonding a counter electrode with a photoanode of the ZnO/ZnSe/CdSe nanocables. The two electrodes in the solar cell were separated by a 60 μm thick polypropylene spacer, and the internal space of the cell was filled with a polysulfide electrolyte (1.0 M S, 1.0 M Na_2S, and 0.1 M NaOH in deionized water). To minimize performance variation from the photoanodes, we used the same photoanode sample to make the different cells to achieve a fair comparison of the various counter electrodes. The active area of each solar cell is 0.20 cm^2.

2.4. Characterization. Crystallographic information on the CZTS structures was studied with powder X-ray diffraction (XRD, Siemens D-500, Cu Kα radiation). Dimensions, morphologies, crystal lattices, and composition of the CZTS samples were characterized with scanning electron microscopy and energy-dispersive X-ray spectroscopy (SEM and EDX, Philips-XL30 FEG), transmission electron microscopy and selected area electron diffraction (TEM and SAED, CM20 FEG, 200 kV), high-resolution transmission electron microscopy (HRTEM, JEOL JEM-2100F, 200 kV), and electron energy loss spectroscopy (EELS, Gatan Tridiem imaging filter attached to the JEOL TEM). Optical absorption data were recorded with an Agilent 8453 UV−vis spectrophotometer. Raman spectra were measured with a Renishaw 2000 system with a 516 nm excitation source. X-ray photoelectron spectroscopy (XPS) analysis was performed in a VG ESCALAB 220i-XL UHV surface analysis system with a monochromatic Al Kα X-ray source (1486.6 eV). Electrochemical impedance spectroscopy (EIS) was performed in dark using an impedance measurement unit (ZAHNER-elektrik IM6) in the frequency range of 0.1−10^5 Hz with an ac amplitude of 10 mV and an applied bias voltage of 0.8 V between the counter electrode and the working electrode.

3. RESULTS AND DISCUSSION

Figure 1a shows SEM images of the sample prepared by reacting $Cu(NO_3)_2$, $Zn(NO_3)_2$, $SnCl_4$, and S in a TEG solvent

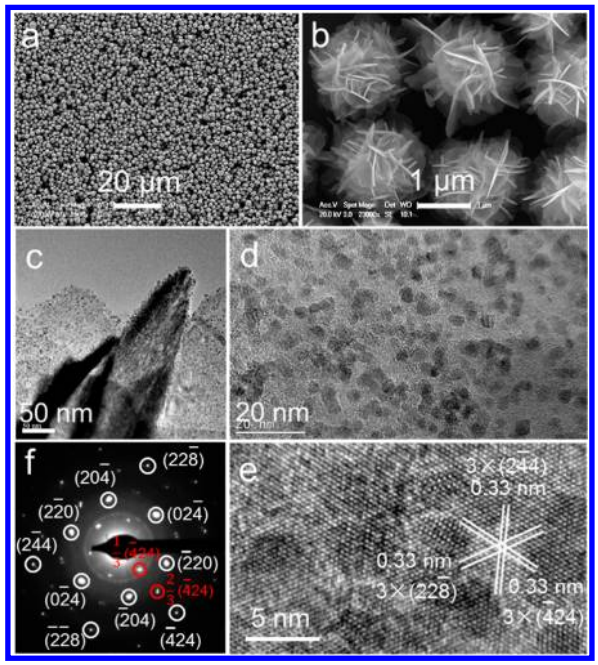

Figure 1. (a, b) SEM images of CZTS microspheres, (c, d) TEM images of CZTS nanoflakes, (e) SAED pattern of a CZTS nanoflake, and (f) HRTEM image of a CZTS nanoflake.

at 250 °C for 48 h, revealing general morphologies of nearly monodisperse microspheres. The hierarchical microspheres with an average diameter of ∼2 μm are assembled from many nanoflakes as shown in Figure 1b. These hierarchical microspheres are further examined with TEM (Figure 1c). The thickness of these nanoflakes is estimated to be ∼20 nm. The TEM image in Figure 1d reveals the nanoflakes in the microspheres are actually constructed from quantum dots with diameters of 3−5 nm, revealing a three-tiered organization of nanocrystallites to nanoflakes and to microspheres. Figure 1e shows an HRTEM image of a typical nanoflake. It can be seen that the flake consists of many quantum dots of similar orientations. The fringe spacings of 0.33 nm match well to the

dx.doi.org/10.1021/jp306628m | J. Phys. Chem. C 2012, 116, 19718−19723

interplanar spacings of the 3 × (22$\bar{8}$), 3 × ($\bar{4}$24), and 3 × (2$\bar{4}$4) planes of tetragonal CZTS. A typical SAED pattern (Figure 1f) of a flake shows only one set of diffraction spots, confirming that the quantum dots in one flakes do have almost the same orientation. The SAED pattern shown in Figure 1f can be indexed to a tetragonal CZTS structure with a zone axis of [221]. Forbidden spots of $^{1}/_{3}$ × ($\bar{4}$24) and $^{2}/_{3}$ × ($\bar{4}$24)planes are also observed and believed to be results of stacking fault in the tetragonal structure, which is similar to the report on tetragonal $CuInSe_2$.[28]

Phase composition of the sample was further examined with XRD and Raman analysis. Figure 2a shows an XRD pattern of

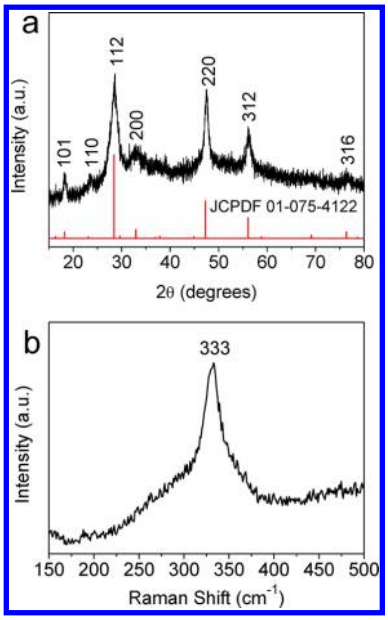

Figure 2. (a) XRD pattern and (b) Raman spectrum of the CZTS microspheres.

the sample prepared by reacting $Cu(NO_3)_2$, $Zn(NO_3)_2$, $SnCl_4$, and S in TEG at 250 °C for 48 h. All the diffraction peaks match well to those of kesterite Cu_2ZnSnS_4 (JCPDF No. 01-075-4122). No diffraction peaks of any impurities can be detected. Figure 2b shows a Raman spectrum of the CZTS microspheres. A peak located at 333 cm^{-1} is observed, which is consistent with the reported values (333−338 cm^{-1}) of the characteristic peak of kesterite CZTS.[29−31] Characteristics peaks from the other impurities such as binary and ternary sulfides are not observed.

X-ray photoelectron spectroscopy (XPS) analysis was used to confirm the presence of the four constituent elements in the sample. Figure 3a shows a Cu 2p core level XPS spectrum of the microspheres. There are two peaks located at 952.24 and 932.17 eV, respectively, with a peak separation of 19.85 eV, indicating the formation of Cu^{+}.[18,32] The Zn 2p peaks at 1045.30 and 1022.25 eV suggest the presence of Zn^{2+} (Figure 3b).[18,32] The Sn 3d XPS core level peaks in Figure 3c at 495.35 and 486.91 eV can be attributed to Sn^{4+}.[18,32] Figure 3d shows XPS spectrum of S 2p with two peaks located at 162.86 and 161.73 eV with a peak separation of 1.13 eV, which are consistent with the expected values (160−164 eV) of S in sulfide phases.[18,32]

The CZTS microspheres were further characterized by elemental electron energy loss spectroscopy (EELS) mappings and energy dispersive X-ray spectroscopy (EDS) mappings.

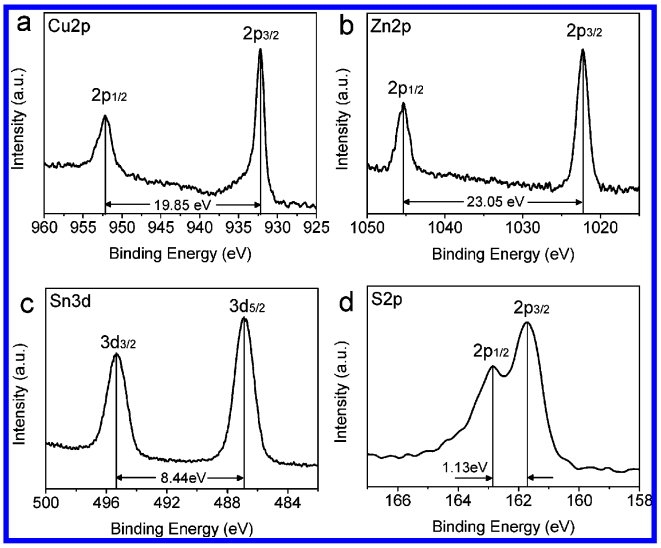

Figure 3. Core level (a) Cu 2p, (b) Zn 2p, (c) Sn 3d, and (d) S 2p XPS spectra of the CZTS microspheres.

Figures 4a−d show respectively Cu, Zn, Sn, and S elemental EELS mappings of a typical nanoflake. The mapping results

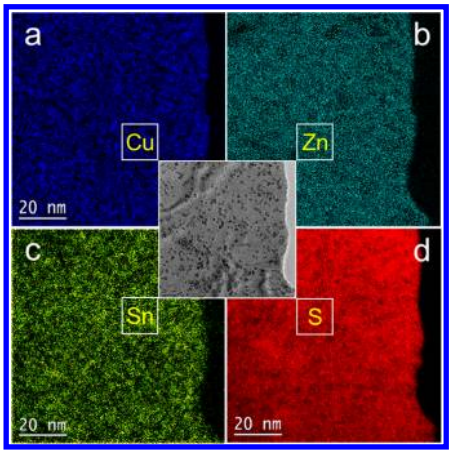

Figure 4. Cu, Zn, Sn, and S elemental EELS mappings of a CZTS nanoflake. Bright-field image of the corresponding nanoflake is shown in the inset.

show that Cu, Zn, Sn, and S are homogeneously distributed throughout the nanoflakes. Consistent with the XRD result, the EDS method also reveals that the atomic ratio of Cu:Zn:Sn:S in our samples is about 28:12:12:48 (Figure S1a), indicating copper-rich CZTS. Figures S1c−f show respectively Cu, Zn, Sn, and S elemental EDS mappings of microspheres shown in Figure S1b, indicating homogeneous distribution of the four constituent elements throughout the microspheres.

Optical absorption properties of the CZTS microspheres were characterized. Figure 5a shows an UV−vis absorption spectrum of the Cu_2ZnSnS_4 microspheres, revealing a broad absorption in visible region. By plotting the $(ahv)^2$−hv (where a = absorbance, h = Planck's constant, and v = frequency) relationship as shown in Figure 5b, the band gap of the CZTS microspheres is estimated to be 1.50 eV, which matches well with the reported values.[17,18,33]

The formation process of the CZTS microspheres has been carefully investigated by XRD, SEM, and Raman analysis, revealing the CZTS microspheres are evolved from CuS

dx.doi.org/10.1021/jp306628m | J. Phys. Chem. C 2012, 116, 19718−19723

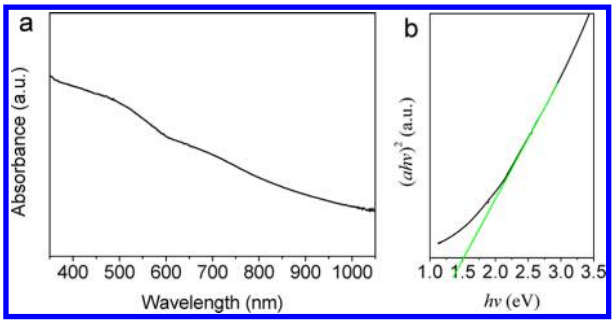

Figure 5. (a) UV–vis absorption spectrum of the CZTS microspheres suspension dispersed in absolute ethanol with concentration of ~0.2 mM. (b) Dependence of $(ahv)^2$ on hv for the CZTS microspheres, revealing a band gap of 1.50 eV.

microspheres. Figures 6a and 6b show the XRD patterns and corresponding Raman spectra of the products obtained at

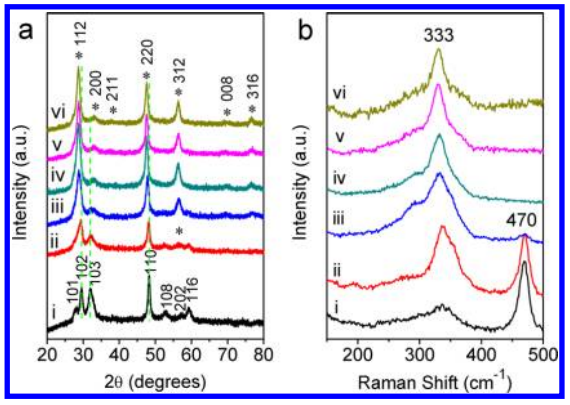

Figure 6. XRD patterns (a) and Raman spectra (b) of the samples obtained by reacting $Cu(NO_3)_2$, $Zn(NO_3)_2$, $SnCl_4$, and S in TEG at 250 °C for different reaction durations: (i) 15 min, (ii) 30 min, (iii) 1 h, (iv) 2 h, (v) 6 h, and (vi) 12 h.

different reaction stages. Curve i in Figure 6a shows the XRD pattern of the product obtained at the reaction time of 15 min. All of the diffraction peaks match well with those of hexagonal CuS (JCPDF No. 06-0464). No diffraction peaks of SnS_2 and ZnS are detected. The corresponding Raman spectrum (curve i in Figure 6b) shows a strong peak located at 470 cm^{-1}, which is consistent with the reported value for CuS,[34] and a weak peak located at 335 cm^{-1}, corresponding to CZTS. When the reaction time is prolonged, both CuS and CZTS phases can be observed. Curves i–iv in Figure 6a evidently reveal that the (102) and (110) diffraction peaks of CuS gradually shift to lower 2θ and evolve respectively into the (112) and (220) peaks of tetragonal CZTS. The diffraction peak (312) of CZTS phase becomes stronger while the (116) and (108) peaks of CuS gradually disappear with longer reaction time. This observation is consistent with the Raman data (curves i–iv in Figure 6b) showing increasing band intensity of the CZTS peak and decreasing band intensity of the CuS peak during this process. When the reaction time reaches 12 h, no CuS phase is detectable. The above results demonstrate that the reaction between S and Cu^{2+} to form binary CuS is much easier to occur than the reaction between S and Sn^{4+} and Zn^{2+} to give binary SnS_2 and ZnS. That is, the formation of SnS_2 and/or ZnS is not favorable in the presence of Cu^{2+}. The as-formed CuS microspheres further react with Sn^{4+} and Zn^{2+} and transform into CZTS microspheres. The corresponding morphology evolution of the hierarchical structures obtained at different reaction stages is shown in Figure S2.

To estimate photovoltaic performance and electrocatalytic activity of CZTS microspheres as a counter electrode material, we fabricate solar cells consisting of the same photoanode of ZnO/ZnSe/CdSe nanocables (Figure S3) and various counter electrodes including bare FTO, Pt/FTO, and CZTS/FTO counter electrodes. Figure 7 shows the current density–voltage

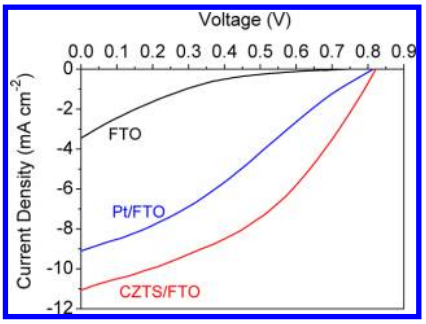

Figure 7. Current density–voltage (J–V) characteristics under illumination of the solar cells constructed from the same photoanode and various counter electrodes of FTO, Pt/FTO, and CZTS/FTO.

(J–V) characteristics of the solar cells, and their key performance parameters are summarized in Table 1. The

Table 1. Photovoltaic Parameters of Solar Cells with Various Counter Electrodes

counter electrode	J_{SC} (mA cm^{-2})	V_{OC} (V)	FF	PCE (%)
FTO	3.46	0.745	0.128	0.33
Pt/FTO	9.11	0.816	0.305	2.27
CZTS/FTO	11.06	0.822	0.410	3.73

device with a bare FTO glass as the counter electrode gives a J_{SC} of 3.46 mA cm^{-2}, a V_{OC} of 0.745 V, and a FF of 0.128, yielding a PCE of 0.33%. Photovoltaic performance is significantly improved by replacing the FTO counter electrode with a Pt/FTO counter electrode. The cell using a Pt/FTO counter electrode gives a J_{SC} of 9.11 mA cm^{-2}, a V_{OC} of 0.816 V, a FF of 0.305, and a PCE of 2.27%. When the CZTS microspheres-coated FTO glass substrate (CZTS/FTO) is employed as a counter electrode, photovoltaic performance of the cell using the same photoanode can be further enhanced. The J_{SC}, V_{OC}, and FF of the cell are increased to 11.06 mA cm^{-2}, 0.822 V, and 0.410, respectively, and resulting in a PCE as high as 3.73%. The above results reveal that CZTS microspheres serve as an effective counter electrode material in QDSSCs using polysulfide electrolyte and contribute to superior performance enhancement including FF, J_{SC}, and PCE.

In our case, these three cells containing the same photoanode and the same polysulfide electrolyte only differ in their counter electrodes. Therefore, the CZTS/FTO counter electrode is considered to provide smaller interfacial recombination between the counter electrode and the polysulfide electrolyte for its enhanced photovoltaic performance (especially the J_{SC}) in comparison with the FTO and Pt/FTO counter electrodes. J_{SC} of the solar cells depends on the series resistance (R_S) of the devices. A smaller R_S is favorable to a higher J_{SC}. R_S of solar cells can be approximately estimated as the inverse of the slopes of the J–V curve at V_{OC}.[35] Therefore, the CZTS/FTO-based solar

dx.doi.org/10.1021/jp306628m | J. Phys. Chem. C 2012, 116, 19718–19723

cell is estimated to show the smallest R_S, which may account for its highest J_{SC}.

R_S of a photoelectrochemical solar cell is associated with the charge transfer resistance (R_{ct}) between counter electrode and electrolyte, and can be expressed as $R_S = R_{TCO} + R_{ct} + R_{diff}$, where R_{TCO} is the substrate resistance and R_{diff} is the diffusion impedance in the electrolyte.[13,36] A smaller R_S suggests a smaller R_{ct} while the same anode and electrolyte are used. Therefore, in our case, the CZTS/FTO counter electrode is suggested to show the smallest R_{ct}. The R_{ct} between counter electrode and electrolyte is typically regarded as an indicator to reveal the electrocatalytic activities of counter electrode materials.[36,37] A smaller R_{ct} facilitates electron transfer from counter electrode to electrolyte for catalytic reduction of S_n^{2-} to S^{2-} and consequently results in less interfacial recombination. Electrochemical impedance spectroscopy (EIS) was used to characterize R_{ct} of the cells. Figure 8 shows Nyquist plots of the

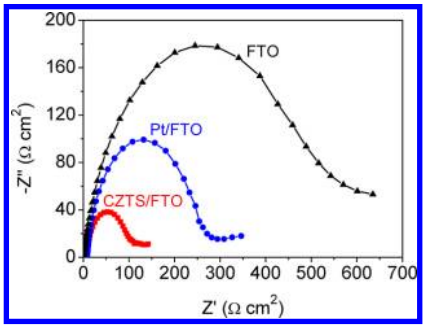

Figure 8. Nyquist plots of solar cells containing the same photoanode of ZnO/ZnSe/CdSe nanocables and various counter electrodes of (a) FTO, (b) Pt/FTO, and (c) CZTS/FTO.

three cells using various counter electrodes. R_{ct} can be estimated from the real impedance component (Z') of the high-frequency semicircles (most left).[13,36,38] The R_{ct} value is decreased from 600 Ω cm^2 for the FTO-based cell to 270 Ω cm^2 for the Pt/FTO-based cell and further to 105 Ω cm^2 for the CZTS/FTO-based cell. This result can well explain the improved photovoltaic performance of the cells using CZTS/FTO counter electrode and also indicates CZTS microspheres show a higher electrocatalytic activity for the reduction of polysulfide electrolyte than noble Pt. Metallic Pt shows better conductivity than the CZTS semiconductor; however, Pt has been reported to show strong absorption of sulfide ions onto its surface to cause surface poison, which results in larger R_{ct} and consequently impairs its catalytic activity.[39] Some binary metal sulfide semiconductors, such as CuS and CoS, have also been demonstrated to show much smaller R_{ct} than metallic Pt counter electrode in QDSSCs using polysulfide electrolyte.[12,13] Our results expand the multinary sulfide family as efficient counter electrode in QDSSCs.

4. CONCLUSIONS

In summary, CZTS hierarchical microspheres with diameters of ~2 μm constructed from nanoflakes with thickness of ~20 nm have been prepared by a one-step solvothermal method. These nanoflakes are assembled from CZTS nanocrystals with diameters of 3−5 nm, revealing a three-tiered organization of the CZTS microspheres with a band gap of 1.50 eV. Their hierarchical structure can provide a high roughness factor, which favors their electrocatalytic performance. In comparison with the noble Pt, the CZTS microspheres show superior electrocatalytic activity for the catalyzing reduction of polysulfide electrolyte, and serve as an effective counter electrode material for low-cost QDSSCs, contributing to obvious improvement in J_{SC} and FF. The solar cell using a CZTS/FTO counter electrode achieves a PCE of 3.73% with a J_{SC} of 11.06 mA cm^{-2} and a V_{OC} as high as 0.822 V, which shows a 64.3% enhancement in PCE compared with the cell using a Pt/FTO counter electrode.

■ ASSOCIATED CONTENT

Supporting Information

EDS spectrum and mappings of CZTS microspheres; SEM images showing the formation process of the CZTS microspheres; SEM image of an array of ZnO/ZnSe/CdSe core/shell nanocables. This material is available free of charge via the Internet at http://pubs.acs.org.

■ AUTHOR INFORMATION

Corresponding Author

*E-mail: apcslee@cityu.edu.hk.

Notes

The authors declare no competing financial interest.

■ ACKNOWLEDGMENTS

This project has been financially supported by Research Grants Council of HKSAR (No. CityU 101910).

■ REFERENCES

(1) Liu, B.; Zeng, H. C. *J. Am. Chem. Soc.* **2005**, *127*, 18262−18268.
(2) Tang, Z.; Kotov, N. A. *Adv. Mater.* **2005**, *17*, 951−962.
(3) Dong, Z.; Lai, X.; Halpert, J. E.; Yang, N.; Yi, L.; Zhai, J.; Wang, D.; Tang, Z.; Jiang, L. *Adv. Mater.* **2012**, *24*, 1046−1049.
(4) Zhang, W.; Li, M.; Wang, Q.; Chen, G.; Kong, M.; Yang, Z.; Mann, S. *Adv. Funct. Mater.* **2011**, *21*, 3516−3523.
(5) Qi, X.; She, G.; Liu, Y.; Mu, L.; Shi, W. *Chem. Commun.* **2012**, *48*, 242−244.
(6) Zhu, T. J.; Li, J.; Wu, Q. S. *ACS Appl. Mater. Interfaces* **2011**, *3*, 3448−3453.
(7) Hwang, Y. J.; Wu, C. H.; Hahn, C.; Jeong, H. E.; Yang, P. *Nano Lett.* **2012**, *12*, 1678−1682.
(8) Liu, J. Y.; Luo, T.; Meng, F. L.; Qian, K.; Wan, Y. T.; Liu, J. H. *J. Phys. Chem. C* **2010**, *114*, 4887−4894.
(9) Wang, L. L.; Fei, T.; Lou, Z.; Zhang, T. *ACS Appl. Mater. Interfaces* **2011**, *3*, 4689−4694.
(10) Lee, J.-H. *Sens. Actuators, B* **2009**, *140*, 319−336.
(11) Yang, Z.; Chen, C.-Y.; Roy, P.; Chang, H.-T. *Chem. Commun.* **2011**, *47*, 9561−9571.
(12) Yang, Z.; Chen, C.-Y.; Liu, C.-W.; Chang, H.-T. *Chem. Commun.* **2010**, *46*, 5485−5487.
(13) Yang, Z.; Chen, C.-Y.; Liu, C.-W.; Li, C.-L.; Chang, H.-T. *Adv. Energy Mater.* **2011**, *1*, 259−264.
(14) Seol, M.; Ramasamy, E.; Lee, J.; Yong, K. *J. Phys. Chem. C* **2011**, *115*, 22018−22024.
(15) Guo, Q.; Hillhouse, H. W.; Agrawal, R. *J. Am. Chem. Soc.* **2009**, *131*, 11672−11673.
(16) Guo, Q.; Ford, G. M.; Yang, W.-C.; Walker, B. C.; Stach, E. A.; Hillhouse, H. W.; Agrawal, R. *J. Am. Chem. Soc.* **2010**, *132*, 17384−17386.
(17) Steinhagen, C.; Panthani, M. G.; Akhavan, V.; Goodfellow, B.; Koo, B.; Korgel, B. A. *J. Am. Chem. Soc.* **2009**, *131*, 12554−12555.
(18) Riha, S. C.; Parkinson, B. A.; Prieto, A. L. *J. Am. Chem. Soc.* **2009**, *131*, 12054−12055.
(19) Ramasamy, K.; Malik, M. A.; O'Brien, P. *Chem. Commun.* **2012**, *48*, 5703−5714.
(20) Xin, X.; He, M.; Han, W.; Jung, J.; Lin, Z. *Angew. Chem., Int. Ed.* **2011**, *50*, 11739−11742.

(21) Dai, P. C.; Zhang, G.; Chen, Y. C.; Jiang, H. C.; Feng, Z. Y.; Lin, Z. J.; Zhan, J. H. *Chem. Commun.* **2012**, *48*, 3006−3008.
(22) Emin, S.; Singh, S. P.; Han, L.; Satoh, N.; Islam, A. *Sol. Energy* **2011**, *85*, 1264−1282.
(23) Kamat, P. V. *J. Phys. Chem. C* **2008**, *112*, 18737−18753.
(24) González-Pedro, V.; Xu, X. Q.; Mora-Seró, I.; Bisquert, J. *ACS Nano* **2010**, *4*, 5783−5790.
(25) Giménez, S.; Mora-Seró, I.; Macor, L.; Guijarro, N.; Lana-Villarreal, T.; Gómez, R.; Diguna, L. J.; Shen, Q.; Toyoda, T.; Bisquert, J. *Nanotechnology* **2009**, *20*, 295204.
(26) Xu, J.; Yang, X.; Yang, Q.-D.; Wong, T.-L.; Lee, S.-T.; Zhang, W.-J.; Lee, C.-S. *J. Mater. Chem.* **2012**, *22*, 13374−13379.
(27) Xu, J.; Yang, X.; Wang, H. K.; Chen, X.; Luan, C. Y.; Xu, Z. X.; Lu, Z. Z.; Roy, V. A. L.; Zhang, W. J.; Lee, C.-S. *Nano Lett.* **2011**, *11*, 4138−4143.
(28) Guo, Q.; Kim, S. J.; Kar, M.; Shafarman, W. N.; Birkmire, R. W.; Stach, E. A.; Agrawal, R.; Hillhouse, H. W. *Nano Lett.* **2008**, *8*, 2982−2987.
(29) Fernandes, P. A.; Salomé, P. M. P.; da Cunha, A. F. *Thin Solid Films* **2009**, *517*, 2519−2523.
(30) Liu, F.; Li, Y.; Zhang, K.; Wang, B.; Yan, C.; Lai, Y.; Zhang, Z.; Li, J.; Liu, Y. *Sol. Energy Mater. Sol. Cells* **2010**, *94*, 2431−2434.
(31) Zhou, Y.-L.; Zhou, W.-H.; Li, M.; Du, Y.-F.; Wu, S.-X. *J. Phys. Chem. C* **2011**, *115*, 19632−19639.
(32) Dai, P. C.; Shen, X. N.; Lin, Z. J.; Feng, Z. Y.; Xu, H.; Zhan, J. H. *Chem. Commun.* **2010**, *46*, 5749−5751.
(33) Yang, X.; Xu, J.; Xi, L. J.; Yao, Y. L.; Yang, Q. D.; Chung, C. Y.; Lee, C.-S. *J. Nanopart. Res.* **2012**, *14*, 931.
(34) Rudigier, E.; Barcones, B.; Luck, I.; Jawhari-Colin, T.; Pérez-Rodríguez, A.; Scheer, R. *J. Appl. Phys.* **2004**, *95*, 5153−5158.
(35) Moliton, A.; Nunzi, J.-M. *Polym. Int.* **2006**, *55*, 583−600.
(36) Ramasamy, E.; Lee, W. J.; Lee, D. Y.; Song, J. S. *Electrochem. Commun.* **2008**, *10*, 1087−1089.
(37) Fabregat-Santiago, F.; Bisquert, J.; Palomares, E.; Otero, L.; Kuang, D.; Zakeeruddin, S. M.; Grätzel, M. *J. Phys. Chem. C* **2007**, *111*, 6550−6560.
(38) Tian, H.; Gabrielsson, E.; Yu, Z.; Hagfeldt, A.; Kloo, L.; Sun, L. *Chem. Commun.* **2011**, *47*, 10124−10126.
(39) Mora-Seró, I.; Giménez, S.; Moehl, T.; Fabregat-Santiago, F.; Lana-Villareal, T.; Gómez, R.; Bisquert, J. *Nanotechnology* **2008**, *19*, 424007.